CrossMark

PAPER IN FOREFRONT

Succinic anhydride functionalized microcantilevers for protein immobilization and quantification

Gianluca Palmara[1] · Alessandro Chiadò[1] · Roberta Calmo[1] · Carlo Ricciardi[1]

Abstract Microcantilever-based systems have been proposed as sensing platforms owing to their high sensitivity when used as mass sensors. The controlled immobilization on a surface of biomolecules used as recognition elements is fundamental in order to realize a highly specific and sensitive biosensor. Here, we introduce for the first time the application to a microcantilever-based system of a reliable chemical functionalization consisting of silanization with an aminosilane followed by a modification resulting in a carboxylated thin film. This chemical functionalization was tested for reproducibility of molecule deposition and for its protein grafting ability. Finally, this system was employed for the quantification of grafted proteins on the microcantilever surface. Moreover, a theoretical surface density of immobilized proteins estimated with bioinformatics tools was compared with the experimental surface density data, providing information about the orientation that the biomolecules assumed with respect to the sensing surface.

Keywords Microcantilever · Chemical functionalization · Protein immobilization · Biosensor · Surface density · Protein orientation

✉ Gianluca Palmara
  gianluca.palmara@polito.it

[1] Department of Applied Science and Technology, Politecnico di Torino, Corso Duca degli Abruzzi 24, 10129 Torino, Italy

Introduction

In the past decades, different transducing principles (i.e., electrochemical, optical, piezoelectric, acoustic, thermal) were applied to biosensing platforms with the aim of increasing the measurement sensitivity to a target substance [1]. Indeed, the selective recognition of specific analytes in different matrices is of fundamental importance in several fields and applications (e.g., clinical diagnostics, environmental monitoring, food control, and foodborne diseases prevention) [1–3]. Moreover, these kinds of applications strongly need a label-free detection to reduce the cost and complexity of the final biosensor.

Microcantilevers (MCs), a class of nanomechanical sensors, are highly sensitive devices capable of label-free quantitative detection of several biomolecules, as they can be functionalized with a number of different biorecognition molecules (nucleic acids, antibodies, and other proteins) [2, 4, 5]. In general, MCs can be used in two operating modes: static mode and dynamic mode [6, 7]. In the former mode, MCs are used as surface stress sensors measuring the deflection induced by the binding of target molecules to the bioreceptors immobilized on the MC surface; in the latter mode, MCs are used as a weighing device (microbalance) using the shift in their resonant frequency to detect the mass of the objects tethered to the MC surface.

In recent years, static mode MCs biosensors have demonstrated detection of different analytes. For instance, they have been applied to sense peptide derived from yeast transcription factor at nanomolar concentrations through the immobilization of a single-chain antibody [5], or to simultaneously detect creatine kinase and myoglobin at a concentration of about 20 μg/mL in a liquid cell [8]. Sensors for DNA transcription factors have also been designed, using MCs functionalized with double-stranded DNA [9], and a femtomolar range sensitivity has been reported measuring the nanomechanical response of nucleic acid films upon controlled hydration conditions [10].

In dynamic mode, systems capable of detecting masses in the femtogram to zeptogram range (10^{-15}–10^{-21} g) have been reported [11–13]. This high sensitivity can be relevant especially for early medical diagnosis. The quantitative detection of prostate specific antigen (PSA) and C-reactive proteins (CRP) in clinical ranges has been reported [14, 15]. In addition, the detection of angiopoietin-1, a tumor biomarker, was performed by characterizing the first and second flexural modes of MCs in a vacuum [16]. The same microcantilever-based approach was successfully applied for the detection of small molecules, such as hormones (17β-estradiol), in serum at concentrations lower than 40 ppt [4].

The key to the success of all of these biosensing devices is the controlled and stable immobilization of proteins, antibodies, or other biomolecules on the surface of biosensors. The proper coverage of sensor surfaces with protein molecules is a challenging but important aspect especially to generate densely packed monolayers of oriented receptors on the sensing surface. This is particularly important for a label-free approach, such as a biosensor based on MC arrays, generally chemically functionalized by self-assembling [17]. The formation of a covalent bond and/or the use of a cross-linking agent is usually applied to obtain a stable immobilization of biorecognition molecules [18, 19].

In this work, a chemical functionalization that consists in the deposition of an amino-terminated film by self-assembly of (3-aminopropyl)triethoxysilane (APTES) and the modification of these terminal amine groups into carboxyl groups (–COOH) by incubation in succinic anhydride (SA) was applied to an MC-based system for the first time. These exposed carboxyl groups are then activated using the cross-linker 1-ethyl-3-(3-dimethylaminopropyl)carbodiimide (EDC) and sulfo-N-hydroxysuccinimide (sulfo-NHS). In the presence of both compounds, the carboxyl groups become sulfo-NHS ester intermediates, which can react with amine nucleophiles with the formation of a stable amide linkage. The EDC/sulfo-NHS activation is a commonly used method for bioconjugation, cross-linking, labeling, and immobilization purposes [20]. This proposed method (APTES/SA) was compared to a widely used chemical functionalization consisting in the deposition of APTES, followed by incubation with glutaraldehyde (GA) (APTES/GA) [2, 18]. Different MC arrays were derivatized and compared in terms of bound molecules by the characterization of MC flexural modes of vibration. At the same time, a theoretical surface density of the grafted molecules was estimated by means of bioinformatics tools. APTES/SA-derivatized MC arrays were then incubated with protein G (PtG), characterized by measuring the frequency shifts, and incubated in bovine serum albumin (BSA). PtG was chosen as a model protein because it has been widely used as an antibody-orienting protein [2, 21]. In fact, the IgG binding domains of PtG are responsible for the specific interaction with the Fragment crystallizable (Fc) region of this class of antibodies. On the other hand, BSA was incubated after PtG immobilization on MC surfaces as a blocking agent. The quantification of the grafted biomolecules was performed from the gravimetric data and compared with a theoretical surface density calculated with the same bioinformatics approach.

APTES/SA proved to be a stable and reproducible functionalization, allowing the formation of a protein adlayer close to an ideal monolayer on the MC surface. Moreover, on the basis of acquired data, it was possible to hypothesize the potential orientation of proteins tethered to the MC sensing surface. Such system paves the way towards quantitative, more specific and stable label-free biosensors owing to a deeper control and understanding of protein–surface interactions.

Materials and methods

Reagents

Recombinant protein G (PtG) and recombinant horseradish peroxidase-conjugated protein G (PtG-HRP) were from Thermo Scientific (Fischer Scientific, Milan, IT). Water used during each step was ultra-pure water dispensed from a DirectQ-3UV Merck-Millipore (Milan, Italy). (3-Aminopropyl)triethoxysilane (APTES, anhydrous, 99 %), glutaraldehyde (GA, 25 % in H_2O), succinic anhydride (SA, 99 %), toluene (anhydrous, 99.8 %), tetrahydrofuran (THF, 99.9 %), triethylamine (TEA), sodium cyanoborohydride (95 %), 2-(N-morpholino)ethanesulfonic acid (MES, 99.5 %), boric acid (99 %), sodium chloride (99.5 %), sulfuric acid (95-97 %, w/w), hydrogen peroxide (30 %, w/w), 3,3',5,5'-tetramethylbenzidine (TMB), 1-ethyl-3-(3-dimethylaminopropyl)carbodiimide (EDC, 99 %), N-hydroxysulfosuccinimide sodium salt (sulfo-NHS, 98 %), Dulbecco's phosphate buffer saline (PBS), polyoxyethylene-glycol-sorbitan monolaurato (Tween-20™), and bovine serum albumin (BSA, protease free, 98 %) were purchased from Sigma Aldrich (Milan, Italy) and used without further purification.

MC fabrication and measurement setup

Arrays of MCs were fabricated starting from a silicon-on-insulator (SOI) wafer, using photolithography and micromachining techniques. The fabrication process is described in detail elsewhere [22]. Briefly, the geometry on the backside of the wafer was defined through optical lithography before performing buffered oxide etch (BOE) to transfer the resist pattern to the oxide layer. Then, ProTEK™ polymer was spin-coated on the front side to protect the surface during the subsequent KOH wet etching of the bulk silicon. Analogously, optical lithography was used to define the planar geometry of MC structures and a reactive ion etching (RIE) process was performed on the silicon device layer. Finally, the release of

MCs was realized through BOE etching of the buried SiO_2 layer. Each array comprises 11 MCs with dimensions of 460 µm in length, 50 µm in width, and 6.5 µm in thickness. Each MC vibrates at a different resonant frequency as a result of the dimension tolerances of the fabrication process that cause each MC to have a slightly different mass. The resonant frequency of the MCs used in this work is in the range 49.2 $\pm$ 3.8 kHz for the first mode and 307.8 $\pm$ 23.5 kHz for the second mode of vibration. The Q-value for the first mode is ca. 50 k, while the Q-value for the second mode is ca. 10 k. Representative resonant curves of the first and second mode of vibration of MCs are reported in Fig. S2 in the Electronic Supplementary Material (ESM). A piezoelectric disk (PI ceramic) was used as actuation system. In order to control the frequency of the vibration, a sinusoidal signal sent to the disk was produced by a lock-in amplifier (HF2LI lock-in amplifier, Zurich Instruments). The MCs were attached to the actuator with double-sided tape, and a vacuum chamber was evacuated to ultrahigh vacuum (UHV) pressure (ca. 5×10^{-6} mbar) by a series of membrane and turbo-molecular pumps (MINI-Task System, Varian Inc. Vacuum Technologies). Finally, the temperature of the vacuum chamber is maintained at 22 °C by means of a Peltier cell. The microcantilever resonant frequency was measured with the optical lever technique in which the position of a laser beam reflected off the top side of the cantilever is monitored by a position-sensitive detector (PSD). The current output of the PSD was amplified and converted into a voltage signal, sent to the lock-in amplifier for signal filtering, and stored in a PC. The measurement process was performed under a LABVIEW environment, and data were fitted with a Lorentzian curve.

Statistical analysis of data

The measurements consisted in characterizing the first and second flexural modes of MCs in vacuum.

For each MC the first and the second flexural modes of vibration are measured, reported as f_i^n where $i = 1, 2$ indicates the modal number (the first and the second mode, respectively), while $n = 1–11$ indicates the MC position in each array. The combination of these two measurements allows one to increase the number of statistical data points. In order to compare measurements from the different vibrational modes, the relative frequency shifts are calculated and defined as

$$\delta_i^n = \frac{\Delta f_i^n}{f_i^n}$$

These two relative shifts related to the two vibrational modes are combined to obtain the arithmetical mean and the half deviation, which are used as the signal of the single cantilever and relative uncertainty, respectively:

$$\delta_{1,2}^n = \frac{\delta_1^n + \delta_2^n}{2}$$

$$\sigma_{\delta_{1,2}^n} = \frac{\left|\delta_1^n - \delta_2^n\right|}{2}$$

The last step consists in the statistical combination of the 11 MCs comprising an array to obtain a single value with its relative uncertainty. Considering each MC of an array as a single "sensor" able to measure a variable with its uncertainty, it is possible to use the weighted mean to calculate a better estimation of the real value of the array (and its relative uncertainty) as

$$\overline{\delta}_{1,2} = \frac{\sum \delta_{1,2}^n w_{1,2}^n}{\sum w_{1,2}^n}$$

$$\sigma_{\overline{\delta}_{1,2}} = \frac{1}{\sqrt{\sum w_{1,2}^n}}$$

where $w_{1,2}^n = \frac{1}{\sigma_{\delta_{1,2}^n}^2}$ is the statistical weight, the function which allows one to attribute a weight to the single data in the calculation of the mean. Using the following equation, it is possible to relate the shift of the eigenfrequency value Δf to the corresponding mass increment Δm:

$$\frac{\Delta f}{f_0} = -\frac{1}{2}\frac{\Delta m}{m_0}$$

where f_0 is the resonant frequency and m_0 is the initial effective mass of the resonator. This relationship is valid if the added mass is uniformly distributed on the MC surface and if the beam spring constant k remains constant after binding of molecules. These assumptions hold for the detection of biomolecules because stiffness and surface stress would likely have a negligible influence on the vibrational behavior of the silicon resonators [21, 23]. Since the frequency variation due to mass loading is dependent on the axial distribution, the relative frequency shifts of different modes of vibration can be an indication of the non-uniform distribution of the molecules on the MC surface. Therefore, since the uncertainty of each MC is here given by the difference in the relative frequency shift of the first versus the second flexural mode, the higher the discrepancy is, the lower the weight of such a MC will be in the final value.

The same weighted mean method was used for the estimation of a single Δm value starting from the data acquired from five MC arrays.

Theoretical estimation of grafted biomolecules densities

Marvin Sketch (6.1.7, 2014, ChemAxon http://www.chemaxon.com) was used to draw and calculate the theoretical geometrical descriptors of the molecules used during the experiments by means of the geometry tool, as

reported elsewhere [24]. The Geometry Descriptors plug-in (v.5.3.2) was used to estimate the following parameters of molecular geometry from structures rendered in three dimensions as the lowest energy conformer and according to van der Waals atomic radii: (1) smallest/largest molecular surface (in angstroms squared) projected from the three-dimensional structure; (2) molecular length measured perpendicularly to this plane of projection (in angstroms); (3) molecular volume (in angstroms cubed). The same approach was applied to proteins. The starting structure for the calculation of the BSA parameters was the PDB 4F5S, while for PtG, the protein model structure was obtained by homology modeling by means of the I-TASSER Web server [25, 26]. A manual evaluation of the projection areas was performed for comparison purposes. Two atoms lying on the same plane of the biomolecule PDB structures were identified using the Viewing Controls-Side View tool of UCSF Chimera (1.10.1, build 40427) [27]. The Distances tool was then used to draw and calculate the distance between the previous selected atoms on the model. Afterward, the surface was displayed and an image was exported for calculations. In order to calculate the theoretical projection area of the biomolecule, this image was finally analyzed with ImageJ [28] by setting the scale using the previously drawn distance. The obtained values of projection areas were used to calculate the theoretical minimal and maximal surface densities of immobilized biomolecules. These theoretical values were compared to the experimental ones obtained with the characterization of MC arrays.

PtG and BSA dimensions were related by calculating a BSA/PtG area ratio, equal to 2.24. Two ratios were calculated: one considering the maximum projection area of the two proteins (2.38) and one considering the minimum projection area (2.11). Finally, the arithmetic mean of these two ratios (2.24) was taken into account because of the impossibility to determine the actual spatial orientation of the two proteins. PtG_{eq} was calculated by multiplying the experimental BSA molecules/cm^2 by the BSA/PtG area ratio.

Chemical functionalization

After the MC fabrication process, a silicon oxide (SiO_2) film of 180 nm was grown on the surface by thermal oxidation in a Tempress furnace at 1100 °C in O_2 atmosphere for 3 h, with heating and cooling rates of 10 °C/min and 2 °C/min, respectively. Afterwards, MC arrays were chemically functionalized by applying two different surface chemical modifications: a recently presented protocol based on APTES/SA [29] and a previous method based on APTES/GA [17]. Briefly, MCs were cleaned in a piranha solution and silanized with a 1 % (v/v) solution of APTES in anhydrous toluene at 70 °C for 10 min. APTES/SA samples were obtained by incubation in a solution of THF containing 50 mM succinic anhydride and 5 % TEA for 2 h at room temperature [29], whereas APTES/

GA samples were incubated for 1 h in a 1 % glutaraldehyde solution in 100 mM borate buffer, pH 8.5, at room temperature. The same functionalization processes were applied to macro samples (silicon squared 5×5 mm^2).

APTES/SA samples were activated using the protocol reported by Chiadò et al. [29]. Briefly, samples were equilibrated in MES buffer (100 mM MES, 0.9 % NaCl, pH 4.7) for 15 min, then incubated in a mixture of EDC (4 mM) and sulfo-NHS (10 mM) in MES buffer for 15 min. Subsequently, samples were rinsed three times in PBS with 0.05 % Tween-20™ (PBS-t) to remove the excess of EDC and sulfo-NHS. Finally, samples were incubated with biomolecules.

MC protein incubation

Functionalized and activated MC arrays were incubated overnight at 4 °C with 50 μL of 50 mg/L of PtG dissolved in PBS-t. Negative controls (blank) were incubated with 50 μL of PBS-t. Subsequently, MCs were rinsed three times with PBS-t and three times with Milli-Q™ grade water. After performing resonant frequency characterization, we incubated MC arrays for 1 h at 22 °C with 50 μL of BSA 10 g/mL dissolved in PBS. Negative controls (blank) were incubated with 50 μL of PBS. Then, the samples were rinsed three times in PBS-t and three times with Milli-Q™ grade water.

Results and discussion

Evaluation of deposition of APTES/GA and APTES/SA molecules on MC arrays

In this work, the APTES/SA protocol was applied to MC arrays as a chemical functionalization able to covalently graft biomolecules on the MC surface with the aim of realizing better performing biosensors. This method was characterized from a physicochemical point of view by means of compositional and morphological surface analysis, demonstrating a higher homogeneity, reproducibility, and stability when compared to the APTES/GA [29].

MC arrays were used as a mass sensor to directly quantify the number of APTES/GA and APTES/SA molecules tethered to their surface after the derivatization processes. In order to estimate the surface densities in the case of a perfect monolayer deposition, theoretical values were calculated by means of the geometrical descriptor tool of Marvin Sketch (see "Theoretical estimation of grafted biomolecules densities"). The theoretical areas covered by molecules (Table 1) were used to make a comparison with the experimental MC data (Table 2).

Ten MC arrays were silanized with APTES: five of them were subsequently incubated with GA, while the five remaining arrays were incubated with SA. In Fig. 1, the mean relative frequency shift of each MC array is reported.

Table 1 Geometrical descriptors of APTES/GA, APTES/SA, PtG, and BSA monolayers calculated using Marvin Sketch's plug-in

	Molecular weight (Da)	Min molecule area (Å^2)	Max molecule area (Å^2)
APTES/GA	234.31	25.34	/*
APTES/SA	234.26	25.34	/*
PtG	21,600.00	1359.91	1721.12
BSA	66,432.90	2864.03	4088.50

Note that APTES/GA and APTES/SA molecular weights were calculated starting from APTES without ethoxy groups

*It is assumed that APTES molecules arrange themselves upward

A quantitative evaluation of the molecules surface density would require a perfect characterization of the surface morphology of each MC. Indeed, such morphology can be slightly different from MC to MC as a result of intrinsic surface defects and non-uniform loading caused by the random diffusion of molecules. The approach used in this work (see "Statistical analysis of data") aims at minimizing the impact due to slightly different surface morphologies of individual MCs owing to the evaluation of the mean mass variation, calculated over the 11 MCs composing each array (see "Statistical analysis of data").

The experimental mean surface density of the five APTES/GA arrays was $(25.81 \pm 16.23) \times 10^{14}$ molecules/cm^2, while the experimental mean surface density of the five APTES/SA arrays was $(3.53 \pm 0.82) \times 10^{14}$ molecules/cm^2. These data highlighted that the measured APTES/SA surface density is in very good agreement with the theoretical value for a monolayer deposition of molecules (3.95×10^{14} molecules/cm^2), while the same value for APTES/GA functionalization is about seven times higher than the expected one. To facilitate a graphical comparison, the relative frequency shift value expected for a perfect monolayer deposition of molecules is added as a dashed line in Fig. 1. Moreover, the measured uncertainty of APTES/GA functionalization is ca. 63 % of the signal value, while APTES/SA functionalization has an uncertainty of ca. 23 % of the signal value. These data acquired using our sensitive MC-based array system suggest that the two derivatization processes are quite different in terms of deposition reliability. Therefore, APTES/SA can be considered a more reproducible

Table 2 APTES/GA and APTES/SA theoretical and experimental mean molecules/cm^2

	Experimental mean Δm ($\times 10^{-11}$ g)	Experimental mean molecules/cm^2 ($\times 10^{14}$)	Theoretical molecules/cm^2 ($\times 10^{14}$)
APTES/GA	53.01 ± 33.34	25.81 ± 16.23	3.95
APTES/SA	7.25 ± 1.69	3.53 ± 0.82	3.95

The experimental means Δm were calculated as reported in "Statistical analysis of data"

chemical functionalization compared with APTES/GA. The lower reproducibility of APTES/GA functionalization can be related to polymerization processes of GA that spontaneously occur in aqueous solutions [30]. The results recorded by measuring the deposition of molecules on the MC arrays were supported by a comparative ELISA assay. This test was used to evaluate the grafting ability of the two functionalization methods investigated. The APTES/GA and APTES/SA functionalized samples showed a comparable OD signal, as shown in Fig. S1 in the ESM. However, the relative uncertainty of the former represents ca. 22 % of the signal value, while the latter ones showed only a relative uncertainty of ca. 5 % of the signal value. This result confirms that the APTES/GA protocol is less reliable even from a functionality point of view when compared with the APTES/SA functionalization.

Quantification of PtG molecules surface density

Once we determined the reliability of the APTES/SA functionalization, we used this protocol to perform the quantification of PtG molecules immobilized on MC arrays. After the activation step, the MC arrays were incubated with a PtG (not conjugated with HRP) and their resonant frequencies were acquired. The experimental data were then compared with the theoretical surface densities evaluated with the same bioinformatics approach (see "Theoretical estimation of grafted biomolecules densities"). Although the Marvin Sketch geometrical descriptors plug-in was reported to be used for small molecules [24], it is still feasible to perform a similar analysis on proteins (i.e., PtG). With the aim of validating the application of this analytical tool to bigger molecules, a manual evaluation of the proteins projection areas was performed by means of UCSF Chimera and ImageJ (see "Theoretical estimation of grafted biomolecules densities"). The resulting areas were compared: the manual method showed a higher projection area for both protein orientations with a difference that was roughly 5 % of the value calculated using the Marvin Sketch plug-in. In order to avoid the user-dependent bias of the manual approach, only the values obtained by the automatic plug-in were taken into account (Table 1).

The bar chart in Fig. 2a shows the response of the MC resonators in terms of mean relative frequency shifts. All five MC arrays incubated with PtG showed a signal that is clearly distinguishable from the blank condition (roughly 10–20 times higher) with an experimental mean surface density of $(4.23 \pm 0.75) \times 10^{12}$ molecules/cm^2, thus characterized by a fairly low relative uncertainty (around 5 %). Moreover, the blank signal results are comparable with the instrumental error $\Delta f / f_0$ ca. $\pm 6 \times 10^{-6}$.

When working with MC arrays (i.e., with analytical replications of the same sensor), the precision of the mean value is intrinsically limited by two factors: the random diffusion of biomolecules in the solution, which can lead to variability in
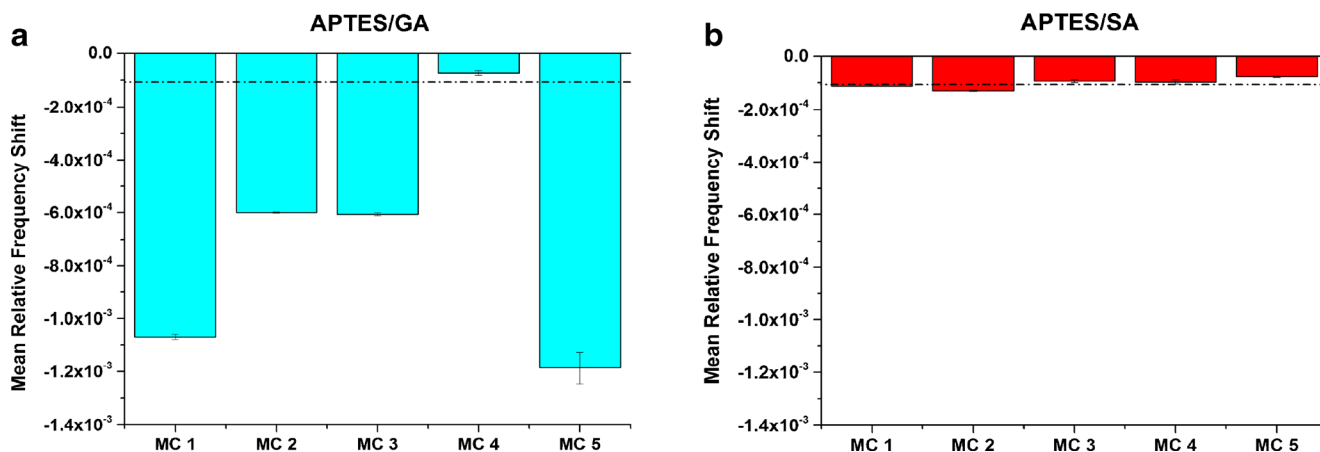
Fig. 1 MC arrays evaluation of APTES/GA and APTES/SA molecules deposition: the bar charts show the mean relative frequency shifts measured after the functionalization processes of APTES/GA (**a**) and APTES/SA (**b**). The mean relative frequency shifts were calculated as reported in "Statistical analysis of data". The *dashed line* represents the relative frequency shift value expected for a monolayer deposition of molecules. Same y-axis was used to facilitate the comparison

transport of the targets to the device sensing area, and the possible orientations that proteins can assume with respect to the surface. As reported by Rabe et al. [31], the orientation of proteins on a surface can be defined as "side-on" or "end-on", considering an elliptically shaped particle that is attached with its long or short axis to the surface. Exposing two different projection areas, these two possible orientations in the space can lead to different protein surface densities (Table 3).

Making a comparison with the theoretical values for PtG-covering areas, we note that the experimental mean surface density is slightly lower than the value expected for a monolayer deposition (between 5.81×10^{12} and 7.35×10^{12} molecules/cm^2), even if it is close to the one corresponding to the theoretical minimum surface density, which is related to a "side-on" immobilization. However, beyond these considerations, there are other aspects to be taken into account. It is well known that proteins fold spontaneously into a three-dimensional structure. The removal of non-polar amino acids from the solvent and their burial into the core of the protein represent the driving force for this folding process [32]. Furthermore, the majority of plasma proteins, such as BSA, are usually able to undergo conformational reorientations upon surface contact and the extent to which proteins can adopt a new conformation is tightly connected to their structural properties, which can be "hard" or "soft" [31]. The amino acid residues in the core of the protein could be involved in the establishment of hydrophobic interactions with surfaces; therefore, the BSA molecules could unfold during the interaction with the MC surface and in this conformation the proteins may assume different projection areas depending on which domain is unfolded. Moreover, the potential establishment of steric hindrance phenomena must be considered. When a protein-containing solution is put in contact with a surface, the protein adlayer structure can be densely or loosely packed
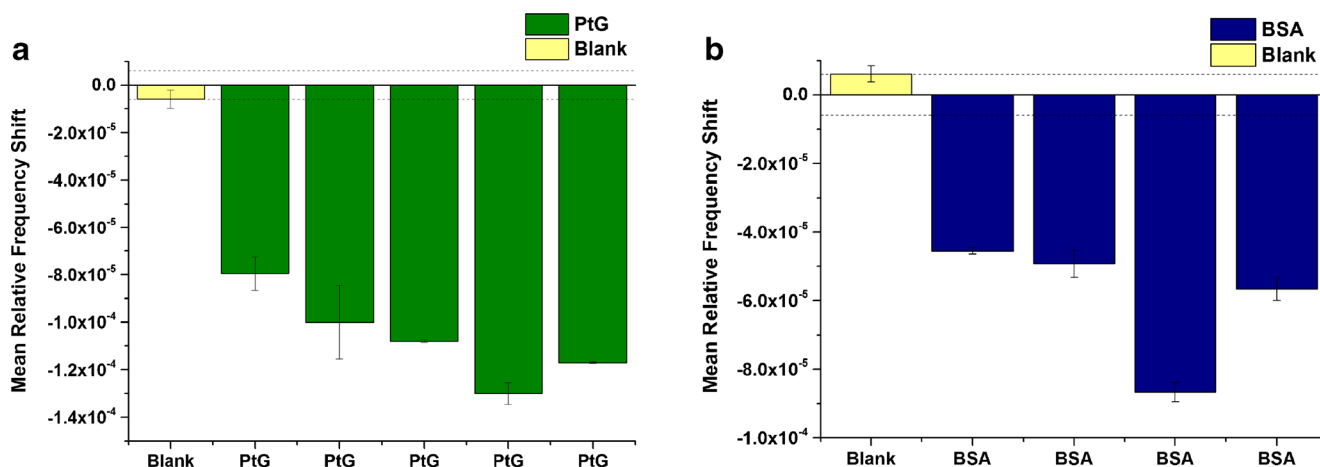

Fig. 2 MC arrays quantification of PtG and BSA: the bar charts show the mean relative frequency shifts measured after the incubation with PtG (**a**) and after the subsequent incubation with BSA (**b**). The *yellow columns* represent the blank condition (incubated with PBS only), while the *dashed line* represents the instrumental error related to the measurement setup. The blank condition in **b** corresponds to the incubation with the saline buffer of the first PtG immobilized MC array (first PtG column from left in **a**)

Table 3 PtG theoretical and experimental mean molecules/cm^2

	Experimental mean Δm ($\times 10^{-11}$ g)		Experimental mean molecules/cm^2 ($\times 10^{12}$)		Theoretical molecules/cm^2 ($\times 10^{12}$)	
	PtG	PtG + PtG$_{eq}$	PtG	PtG + PtG$_{eq}$	Min	Max
Protein G	8.02 ± 1.42	12.23 ± 2.80	4.23 ± 0.75	5.94 ± 1.36	5.81	7.35

The table reports the estimated surface densities (minimum and maximum) and the experimentally measured surface density of PtG. PtG$_{eq}$ represents the BSA molecules/cm^2 converted to PtG molecules/cm^2 using a BSA/PtG ratio and it is calculated as reported in "Theoretical estimation of grafted biomolecules densities"

depending on the chemical properties of proteins (i.e., electrostatic interactions and pI), on the properties of the solution (i.e., pH and ionic strength), and on the physicochemical features of the surface (i.e., wettability, roughness, chemical composition). Therefore, a randomized adsorption of protein on the surface can lead to an inefficiently packed protein layer, leaving undefined gaps between adsorbed proteins, which are not large enough to accommodate another protein [31, 33, 34].

Keeping in mind all these aspects, the investigation of the preferential orientation ("side-on" or "end-on") of the PtG immobilized on the surface was performed. In order to do so, PtG surface residues were analyzed according to the primary amine functionalities or according to the surface electrostatic potential of the amino acids. Those residues with a primary amine are able to react with activated carboxyl groups present on the APTES/SA functionalized surface: the N-terminus and the Lys residues were taken into account for this analysis.

In Fig. 3a, the Lys residues (light blue) and the N-terminus (blue) are shown; in Fig. 3b, the electrostatic potential is represented (negatively charged residues in red and positively charged residues in blue). The images indicate that the majority of Lys are located in proximity of the N-terminus and a region of highly packed negatively charged residues stands at the opposite side of the protein. Therefore, it is more likely that the PtG molecule binds to the chemical functionalization by reacting with one of those residues through a "side-on" immobilization. Moreover, this hypothesis is corroborated by the asymmetrical distribution of negatively charged residues that would contribute to the formation of a loosely packed "side-on" monolayer, as recorded by our PtG quantification.
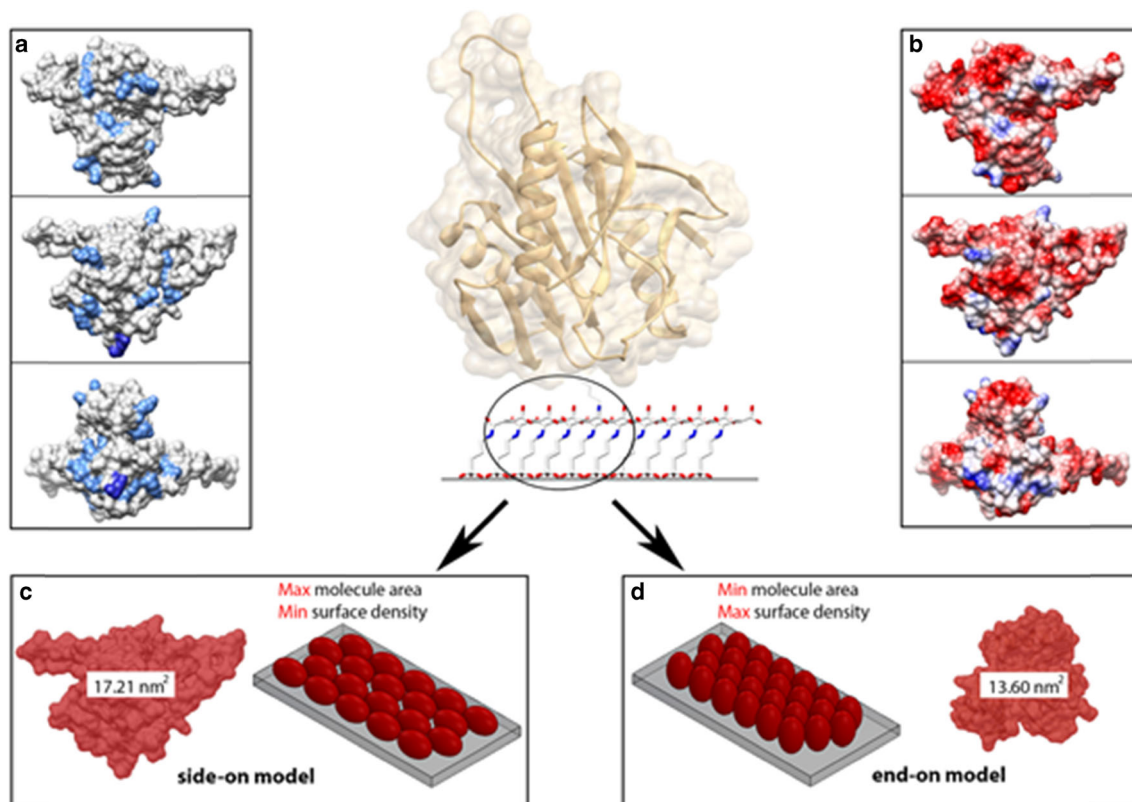

Fig. 3 Amine functionalities (**a**) and electrostatic potential of surface amino acids (**b**) of protein G; protein G "side-on" (**c**) and "end-on" (**d**) orientation models. The Lys residues are in *light blue* and the N-terminus is in *blue*, while negatively charged residues are in *red* and positively charged residues are in *blue*

Experimental data suggest that, in our case, PtG deposited on the MC surface does not achieve a complete monolayer arrangement of proteins and so it is reasonable that areas of chemical functionalization remain available for the potential interaction of other biomolecules. These findings are consistent with the fact that the achievement of a perfect monolayer of proteins on a solid surface is a difficult task that quite often remains an "ideal" concept, rather than a real experimental condition. As an example, Su et al. reported that a submonolayer deposition can be obtained at low concentration of lysozyme, while the formation of a multilayered structure is reached if the concentration is increased [35].

MC arrays were then incubated with BSA. This incubation step represents a saturation of the available surface for BSA binding after the PtG grafting. Subsequently, the resonant frequencies were characterized again to evaluate the actual immobilization of a protein monolayer. The bar chart in Fig. 2b shows the mean relative frequency shifts after BSA incubation. Analogously, each MC array gave a signal proportional to the mass of BSA molecules tethered to MC sensing surfaces and the blank response was again comparable with the instrumental error. The MC array corresponding to the blank condition in the PtG immobilization step is not reported in Fig. 2b: the APTES/SA carboxyl groups were no longer activated after several hours in the BSA incubation step because of the NHS-ester hydrolysis rate in aqueous solution; thus, they represent a less efficient substrate for the covalent immobilization of BSA molecules. Looking at these data, it is possible to notice that the amplitude of frequency shifts varies from one MC array to another. This variability of BSA attachment can be attributed to the cross-section and geometry of the available surface for BSA binding after the PtG deposition. BSA molecules are mainly bound to the sensing surface through electrostatic interactions, while a minor part of them may form covalent bonds because of the low intrinsic reactivity of the APTES/SA carboxyl groups, which are no longer activated. Moreover, it is feasible that the BSA molecules are more able than PtG to saturate the available surface (unoccupied by PtG) because they are incubated at a much larger concentration than PtG (BSA 10 g/L vs. PtG 50 mg/L).

In order to better understand the interaction of the biomolecules with the sensor surface, the PtG and BSA dimensions were related by calculating a BSA/PtG area ratio, corresponding to 2.24, as reported in "Theoretical estimation of grafted biomolecules densities". Afterwards, values of measured BSA molecules/cm^2 were multiplied by this ratio to estimate the equivalent number of PtG molecules/cm^2 (PtG$_{eq}$) and this value was added to the PtG molecules/cm^2 obtained in the previous step. The resulting value of total protein coverage was then compared with the theoretical values of PtG surface density reported in Table 3, corresponding to an ideal monolayer of PtG grafted to the surface. This experimental evaluation, made considering an ideal flat surface model, allowed us

to calculate a surface density value that, once compared to the theoretical one, could provide information about the orientation of the proteins tethered to the MC surface.

The experimental mean PtG + PtG$_{eq}$ surface density of $(5.94 \pm 1.36) \times 10^{12}$ molecules/cm^2 is between the minimum and maximum theoretical surface densities. Notably, this value is very close to the expected value for minimum surface density, indicating that the preferred orientation of the proteins is probably the one exposing the maximum projection area, confirming the "side-on" immobilization of the PtG. Even considering that the MC surface could be not perfectly flat, thus increasing the number of available binding sites, our experimental surface density, close to the minimum theoretical one, further confirms the "side-on" immobilization of the PtG. A similar behavior is reported by Su et al. for the interaction of lysozyme at the silica–water interface [35].

Conclusions

In this work, we reported for the first time the application to an MC-based system of an APTES/SA chemical functionalization followed by EDC/sulfo-NHS activation. From comparative experiments, APTES/SA proved to be a more stable and reproducible functionalization than APTES/GA in terms of proteins grafting ability. The quantification of the immobilized proteins after the incubation with PtG and BSA was performed and compared with a theoretical estimation of molecules/cm^2 needed to obtain a monolayer arrangement. The experimental data revealed a good agreement with the theoretical values, suggesting the formation of a well-packed monolayer. Furthermore, these data provided information about the preferential orientation of adsorbed proteins, allowing us to formulate interesting considerations about the structure of the protein layers arranged on a solid surface. The method proposed here paves the way toward quantitative, more specific and stable biosensors owing to a deeper control and understanding of protein–surface interactions.

Compliance with ethical standards

Disclosure of potential conflicts of interest The authors declare that they have no conflicts of interest.

Research involving human participants and/or animals This work does not contain any studies with human participants or animals.

References

1. Serra P. Biosensors. Vukovar: InTech; 2010.

2. Ricciardi C, Castagna R, Ferrante I, Frascella F, Luigi Marasso S, Ricci A, et al. Development of a microcantilever-based immunosensing method for mycotoxin detection. Biosens Bioelectron. 2013;40:233–9. doi:10.1016/j.bios.2012.07.029.

3. Chiadò A, Varani L, Bosco F, Marmo L. Opening study on the development of a new biosensor for metal toxicity based on pseudomonas fluorescens pyoverdine. Biosensors. 2013;3:385–99. doi:10.3390/bios3040385.

4. Ricciardi C, Ferrante I, Castagna R, Frascella F, Luigi S, Santoro K, et al. Immunodetection of 17beta-estradiol in serum at ppt level by microcantilever resonators. Biosens Bioelectron. 2013;40:407–11. doi:10.1016/j.bios.2012.08.043.

5. Backmann N, Zahnd C, Huber F, Bietsch A, Plückthun A, Lang H-P, et al. A label-free immunosensor array using single-chain antibody fragments. Proc Natl Acad Sci U S A. 2005;102:14587–92. doi:10.1073/pnas.0504917102.

6. Boisen A, Dohn S, Keller SS, Schmid S, Tenje M. Cantilever-like micromechanical sensors. Rep Progr Phys. 2011;74:036101. doi:10.1088/0034-4885/74/3/036101.

7. Johnson BN, Mutharasan R. Biosensing using dynamic-mode cantilever sensors: a review. Biosens Bioelectron. 2012;32:1–18. doi:10.1016/j.bios.2011.10.054.

8. Arntz Y, Seelig JD, Lang HP, Zhang J, Hunziker P, Ramseyer JP, et al. Label-free protein assay based on a nanomechanical cantilever array. Nanotechnology. 2002;14:86–90. doi:10.1088/0957-4484/14/1/319.

9. Huber F, Hegner M, Gerber C, Güntherodt H-J, Lang HP. Label free analysis of transcription factors using microcantilever arrays. Biosens Bioelectron. 2006;21:1599–605. doi:10.1016/j.bios.2005.07.018.

10. Mertens J, Rogero C, Calleja M, Ramos D, Martín-Gago JA, Briones C, et al. Label-free detection of DNA hybridization based on hydration-induced tension in nucleic acid films. Nat Nanotechnol. 2008;3:301–7. doi:10.1038/nnano.2008.91.

11. Ekinci KL, Huang XMH, Roukes ML. Ultrasensitive nanoelectromechanical mass detection. Appl Phys Lett. 2004;84:4469–71. doi:10.1063/1.1755417.

12. Hosaka S, Chiyoma T, Ikeuchi A, Okano H, Sone H, Izumi T. Possibility of a femtogram mass biosensor using a self-sensing cantilever. Curr Appl Phys. 2006;6:384–8. doi:10.1016/j.cap.2005.11.024.

13. Waggoner PS, Craighead HG. Micro- and nanomechanical sensors for environmental, chemical, and biological detection. Lab Chip. 2007;7:1238–55. doi:10.1039/b707401h.

14. Lee JH, Yoon KH, Hwang KS, Park J, Ahn S, Kim TS. Label free novel electrical detection using micromachined PZT monolithic thin film cantilever for the detection of C-reactive protein. Biosens Bioelectron. 2004;20:269–75. doi:10.1016/j.bios.2004.01.024.

15. Wee KW, Kang GY, Park J, Kang JY, Yoon DS, Park JH, et al. Novel electrical detection of label-free disease marker proteins using piezoresistive self-sensing micro-cantilevers. Biosens Bioelectron. 2005;20:1932–8. doi:10.1016/j.bios.2004.09.023.

16. Ricciardi C, Fiorilli S, Bianco S, Canavese G, Castagna R, Ferrante I, et al. Development of microcantilever-based biosensor array to detect Angiopoietin-1, a marker of tumor angiogenesis. Biosens Bioelectron. 2010;25:1193–8. doi:10.1016/j.bios.2009.10.006.

17. Frascella F, Ricciardi C. Functionalization protocols of silicon micro/nano-mechanical biosensors. Methods Mol Biol. 2013;1025:109–15. doi:10.1007/978-1-62703-462-3.

18. Adeloju SB, Lawal AT. Fabrication of a bilayer potentiometric phosphate biosensor by cross-link immobilization with bovine serum albumin and glutaraldehyde. Anal Chim Acta. 2011;691:89–94. doi:10.1016/j.aca.2011.02.020.

19. Shen G, Zhang X, Shen Y, Zhang S, Fang L. One-step immobilization of antibodies for α-1-fetoprotein immunosensor based on dialdehyde cellulose/ionic liquid composite. Anal Biochem. 2015;471:38–43. doi:10.1016/j.ab.2014.09.020.

20. Maraldo D, Mutharasan R. Optimization of antibody immobilization for sensing using piezoelectrically excited-millimeter-sized cantilever (PEMC) sensors. Sens Actuators B Chem. 2007;123:474–9. doi:10.1016/j.snb.2006.09.034.

21. Waggoner PS, Varshney M, Craighead HG. Detection of prostate specific antigen with nanomechanical resonators. Lab Chip. 2009;9:3095–9. doi:10.1039/b907309b.

22. Canavese G, Marasso SL, Quaglio M, Cocuzza M, Ricciardi C, Pirri CF. Polymeric mask protection for alternative KOH silicon wet etching. J Micromech Microeng. 2007;17:1387–93. doi:10.1088/0960-1317/17/7/022.

23. Ricci A, Ricciardi C. A new finite element approach for studying the effect of surface stress on microstructures. Sens Actuators A Phys. 2010;159:141–8. doi:10.1016/j.sna.2010.03.008.

24. Martineau LC. Simple thermodynamic model of unassisted proton shuttle uncoupling and prediction of activity from calculated speciation, lipophilicity, and molecular geometry. J Theor Biol. 2012;303:33–61. doi:10.1016/j.jtbi.2012.02.032.

25. Roy A, Kucukural A, Zhang Y. I-TASSER: a unified platform for automated protein structure and function prediction. Nat Protoc. 2010;5:725–38. doi:10.1038/nprot.2010.5.I-TASSER.

26. Yang J, Yan R, Roy A, Xu D, Poisson J, Zhang Y. The I-TASSER Suite: protein structure and function prediction. Nat Methods. 2014;12:7–8. doi:10.1038/nmeth.3213.

27. Pettersen EF, Goddard TD, Huang CC, Couch GS, Greenblatt DM, Meng EC, et al. UCSF Chimera - a visualization system for exploratory research and analysis. J Comput Chem. 2004;25:1605–12. doi:10.1002/jcc.20084.

28. Schneider CA, Rasband WS, Eliceiri KW. NIH Image to ImageJ: 25 years of image analysis. Nat Methods. 2012;9:671–5. doi:10.1038/nmeth.2089.

29. Chiadò A, Palmara G, Ricciardi S, Frascella F, Castellino M, Tortello M, et al. Optimization and characterization of a homogeneous carboxylic surface functionalization for silicon-based biosensing. Colloids Surf B: Biointerfaces. 2016;143:252–9. doi:10.1016/j.colsurfb.2016.03.048.

30. Migneault I, Dartiguenave C, Bertrand MJ, Waldron KC. Glutaraldehyde: behavior in aqueous solution, reaction with proteins, and application to enzyme crosslinking. BioTechniques. 2004;37:790–802.

31. Rabe M, Verdes D, Seeger S. Understanding protein adsorption phenomena at solid surfaces. Adv Colloid Interface Sci. 2011;162:87–106. doi:10.1016/j.cis.2010.12.007.

32. Pace CN, Shirley AB, Mcnutt M, Gajiwala K. Forces contributing to the conformational stability of proteins. FASEB J. 1996;10:75–83.

33. Hlady V, Buijs J. Protein adsorption on solid surfaces. Curr Opin Biotechnol. 1996;7:72–7.

34. Gray JJ. The interaction of proteins with solid surfaces. Curr Opin Struct Biol. 2004;14:110–5. doi:10.1016/j.sbi.2003.12.001.

35. Su TJ, Lu JR, Thomas RK, Cui ZF, Penfold J. The effect of solution pH on the structure of lysozyme layers adsorbed at the silica - water interface studied by neutron reflection. Langmuir. 1998;7463:438–45.

Gianluca Palmara received his M.Sc. in cellular and molecular biology at the University of Turin, studying the modulation of electrical excitability of immortalized GnRH neurons. He was awarded his Ph.D. in electronic devices at the Polytechnic University of Turin and his research interests are mainly focused on chemical functionalization of silicon devices and biomolecule interactions with nanomechanical microcantilever-based biosensors.
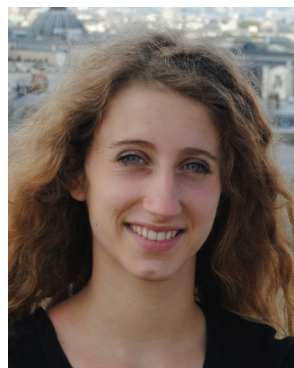
Roberta Calmo received her master's degree in science and technology of bio and nanomaterials from Ca' Foscari University of Venice in 2015. She is currently a Ph.D. student at the Politecnico of Turin in Materials and Processes for Micro and Nano Technologies group of Professor Candido Fabrizio Pirri. Her research is mainly focused on the development and integration of nanomechanical biosensing platform.

Alessandro Chiadò graduated in industrial biotechnolgy at the Università degli Studi di Torino, Italy, in 2009, studying the production of biopolymers by milk whey fermentation. In 2013 he was awarded a Ph.D. in metrology – Industrial safety and risk analysis at Politecnico di Torino, evaluating new biorecognition elements (e.g., engineered enzymes) for environmental monitoring. He is now working on biosensing for medical applications and his current interests are related to the chemical and biological functionalization of different surfaces, to the optimization of bioassay on nanostructured devices, and to the application of bioinformatics to these aspects of biosensors development.

Carlo Ricciardi is Associate Professor in Physics of Condensed Matter at Politecnico di Torino (Italy), where he holds the class of "Micro and nano technology applied to biomedicine, environment and energy". His main research interests are (i) micro/nanomechanical devices for innovative biological and chemical sensors; (ii) synthesis and characterization of nanostructure materials; (iii) memristor-based neuromorphic systems.